Southern Region Engineering Conference
11-12 November 2010, Toowoomba, Australia
SREC2010-xxx *(replace with the reference number of your paper)*

The developments of structural health/integrity monitoring systems using FBG sensors at CEEFC of USQ

Gayan C. Kahandawa, Jayantha A. Epaarachchi, Hao Wang and Thiru Aravinthan
Centre of Excellence in Engineered Fibre Composites
University of Southern Queensland,
Toowoomba, Australia
gayan@usq.edu.au

Abstract—Past few years CEEFC of USQ has been developing SHM systems using novel sensors including Fibre Bragg Grating (FBG) sensors, to monitor structural health/integrity of advanced composite structures. Advanced composite structural componets with embedded FBG sensors have been tested under various loading types in order to understand the the behaviour and spectral responses of embedded FBG sensors at several failure modes of composite materials. This paper details some of the results obtained from few research projects on SHM using FBG sensors which are being undertaken by CEEFC collaboration with the industry.

Keywords-structural health monotoring, FBG sensors, composite materials.

I. INTRODUCTION

Structures made of fibre reinforced polymers (FRP) are widely used in engineering structures such as aircrafts, construction, chemical, civil infrastructures and defense industries. Depending on the application, structural composite components will undergo both static and dynamic loading during their operational lifetime. Exceeding allowed loading and continuous degradation of material properties can cause damages such as cracking of fibre and matrix delamination and unexpected catastrophic failures. Early detection of such damages can be used to prevent further damages to the structure. As such, development of structural health monitoring (SHM) systems to evaluate the damages is a fundamental requirement for the safe operation of modern advance composite structures.

Recent advances in fibre optic sensor technologies have provided great opportunities to develop more sophisticated in-situ SHM systems. There has been a large number of research work on health monitoring of composite structures using Fibre Bragg Grating (FBG) sensors. The ability to embed inside FRP material in between different layers provides the closer look upon defects. The attractive properties such as small size, immunity to electromagnetic fields, multiplexing ability are some of the advantages of FBG sensors. The lifetime of FBG sensor is well above the structures and also it provides the measuring of multiple parameters such as load/strain, vibration and temperature.

Monitoring strain by measuring the wavelength shift of the light reflected from the FBG sensor has often been applied in conventional health monitoring [1,2]. Gumes and Menendez (2002), Barton *et al* (2001), Okabe *et al.* (2002 and 2004), Yashiro *et al.* (2005), Ling *et al.* (2004 and 2006) and Epaarachchi *et al.* (2007 and 2009) have successfully used embedded FBG sensors to measure internal strain and investigated the change of spectral shapes and change of strain in the vicinity of a damage[3-10]. FBG sensors are also sensitive to the strain distributions along the gage sections [11]. Peters et al.[12] (2001) measured reflection spectra in a compact tension specimen with an embedded FBG sensor and simulated the change in the spectrum shape resulting from the large strain gradients. Takeda et al. [13] (2002) first utilized this feature to detect internal damage in CFRP laminates. They reported identification of a delamination using an embedded FBG sensor and pointed that there can be a relationship between delamination length and intensity ratio of the spectrum. Several delamination sizes were investigated near a FBG sensor and using experimental data and theoretical calculations, the sensitivity of a FBG sensor to a stress gradient was confirmed. Building up on these recent advancements of FBG sensor technology, CEEFC of USQ is undertaking various SHM projects using FBG sensors. This paper details some of the achievements of CEEFC in this sense which are being further developed into complete SHM systems for advanced composite structures.

II. FBG SENSORS

K.O. Hill et al. [14] (1978) first observed the formation of a photo-induced grating in a germania-doped optical fiber. Hill´s gratings were made in the fiber core by standing wave of 488nm argon laser light. The grating exposure in this case was shown to be a two-photon process. They have come across 4% back reflection due to variation in refractive index. The field did not progress until Gerry Meltz et al. [15](1989) of United Technologies proposed that fiber gratings could be formed by exposure through the cladding glass by two interfering beams of coherent UV light, thus exciting the 240 nm band directly by one photon absorption. Reliable fabrication of Bragg gratings depends on a detailed knowledge of the underlying mechanisms of photo-induced index changes.

FBG sensors are fabricated in the core region of specially fabricated single mode low-loss germanium doped silicate

optical fibres. The grating is the laser-inscribed region which has a periodically varying refractive index. This region reflects only a narrow band of light corresponding to the Bragg wavelength $\lambda_{B,}$ which is related to the grating period Λ_o [16].

$$\lambda_B = \frac{2n_o \Lambda_o}{k} \qquad (1)$$

Where k is the order of the grating and no is the initial refractive index of the core material prior to any applied strain.

Due to the applied strain, ε, there is a change in the wavelength, $\Delta\lambda_{B,}$ for the isothermal condition,

$$\frac{\Delta\lambda_B}{\lambda_B} = \varepsilon\, P_e \qquad (2)$$

Where P_e is the strain optic coefficient and calculated as 0.793.

The Bragg wavelength is also changing with the reflective index. Any physical change in the fibre profile will cause variation of reflective index. The variation of Bragg wave length λ_B,as a function of change in the refractive index $\Delta\delta n$, and the grating period $\delta\Lambda_o$, is given below.

$$\delta\lambda_{Bragg} = 2\Lambda_o \eta \Delta\delta n + 2n_{eff}\delta\Lambda_o \qquad (3)$$

Where η is core overlap factor of ~0.9 times the shift of Bragg wavelength.

A. Embedding FBG Sensors

The main advantage of FBG sensors is the ability to embed in-between fiber layers. With the requirement, the sensors can be embedded in any layer with any desirable angle. Special care has to be taken to protect the sensor while in fabrication process. There are various fabrication techniques has been developed at CEEFC to avoid pre-mature failures of FBGs during fabrication stages. Figure 1 shows a fabricated composite specimen with an embedded FBG sensor in the middle of the sample.

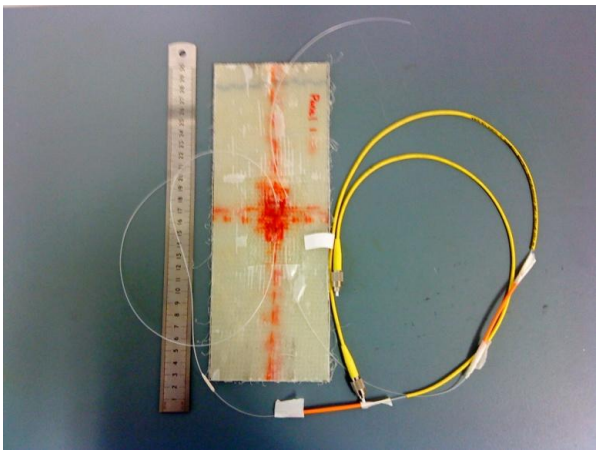

Figure 1. Pannel with an embedded FBG sensors

III. Structural Health Monitoring Projects

A. An Aerospace Component

Most of the aerospace structures undergo complex multi-axial loading while in operation. Monitoring such structures becomes more important to since the probability to failure is comparatively high.

Structural component under torsion and torsion and bending combined loading have been investigated using FBG sensors. FRP tube was fabricated with embedded FBG sensors and with different loading conditions the spectrums were analyzed.

B. Fabrication of The Specimens

FBG sensors which operate in the range of a 1550nm centre wavelength and with the grating length of 10mm were embedded in the two of the specimens. To ensure maximum bonding between FBG sensor and matrix of resin in the GFRP material, the acrylate layer at the grating region of the fibre was removed. Extra protective layer of rubber was applied to the fibre to maximize the handling of samples without damage to the sensors.

Three specimens were prepared using two different lay-up configurations. Specimen 1 is fabricated with four layers of biaxial glass fibre with $90^o\backslash 45^o\backslash 45^o\backslash 90^o$. The specimens 2 and 3 were fabricated with 6 layers of biaxial glass fibre fabric in the orientation of $90^o\backslash 45^o\backslash 45^o\backslash 45^o\backslash 45^o\backslash 90^o$. Kenetix R246TX resin is used as the matrix. The inner diameter of the tube is $\varnothing$ = 50mm and the thickness, $\Delta\varnothing$, is in the range of $\Delta\varnothing$ = 3mm. The dimensions were selected according to the recommended geometry in Ref. 17 for torsion shear testing of thin-walled tubes to ensure the shear stress is uniformly distributed around the circumference and along the axis of the tube. The wall thickness is made small compared to the mean radius so that the through-thickness shear gradient is negligible. The ends of the specimens are over layered with additional layers and tapered to promote failure with in gauge length. The tab thickness is 10mm (Figure 2 and 3).

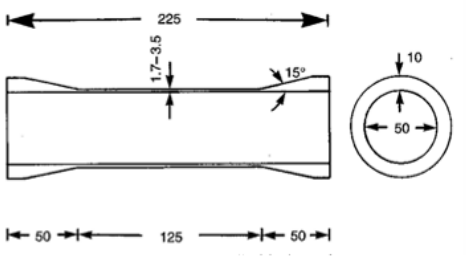

Figure 2. Configuration of the cylicdrilal speciman

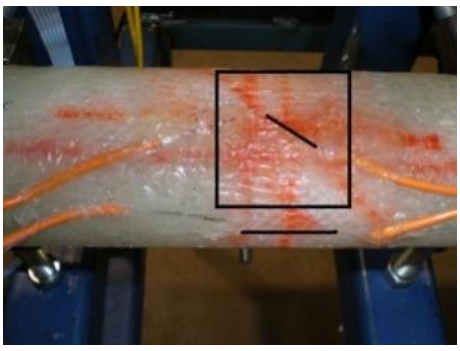

Figure 3. Cylindrical specinams with embedded FBG sensors

C. *Experimentation*

The torsional testing equipment and the test configuration is shown in Figure 4. The torsional testing equipment was designed and manufactured at Centre of Excellence in Engineering Fibre Composites (CEEFC), University of Southern Queensland (USQ). The specimens were mounted on the torsion test machine with one end fixed. The other end of the specimen was supported with roller supports to avoid bending of the samples. Torque is applied by loading the arm attached at the roller support side by means of a screw jack. Applied torque is measured using a S type load-cell with 0-2kN range. The specimen was loaded in the steps of 50Nm, and the strain gauge readings and FBG spectrums were recorded. Vishay Micro-Measurements P3 strain indicator was used to measure the strain and Micron Optics 3.1 sm125 optical spectrum analyser was used to measure FBG spectrum (Figure 5). Each specimen was loaded three times to maintain the reliability of the readings. The data were stored for post processing.

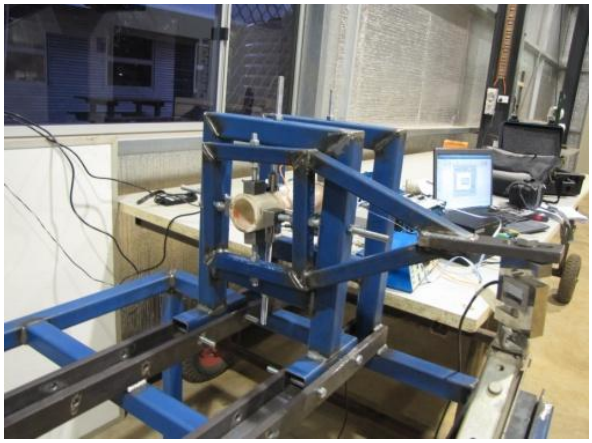

Figure 4. Torsion testing machine

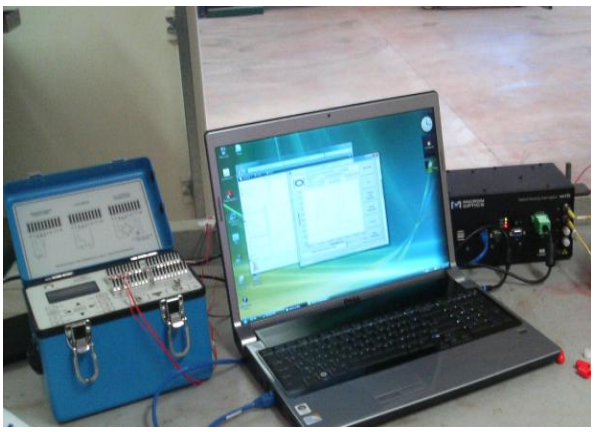

Figure 5. Usual experimental set up FBG readings

D. *Monitoring FRP Bridge Girders*

Two different FRP bridge girders, an I beam and a rectangular beam sections as shown in Figure 6 were designed and fabricated by two industry partners under Queensland Government Smart State project. The basic building blocks of those two sections were pultruted beam sections and phenolic resin cores. In this project major objective was to monitor the integrity of adhesive line between basic building blocks of the girder sections.

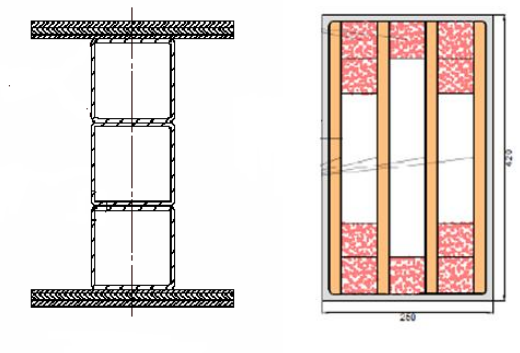

Figure 6. Basic configurations bridge girder of samples

E. *Fabrication of The Specimens*

Two specimens were fabricated to represent the two beam concepts. Specimen 1 was fabricated with an I section as shown in the Figure 7. The beam was fabricated to a length of 1500 mm, using two 300mm x 6mm panels and a 100mm x 75mm pultrusions. The FBG sensors were embedded in the glue layer as shown in Figure 8.

Figure 7. Prototype I beam with embedded FBG sensors

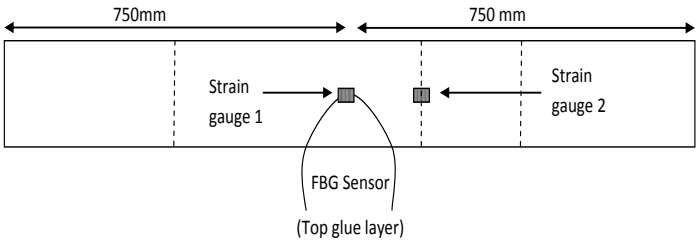

Figure 8. Placement of FBG sensors in I Beam

The specimen 2 was with a rectangular cross section. Two pultrusions were glued in-between two panels as shown in Figure 10. 50x50mm pultrutions with the thickness of 5 mm and panels with 20mm thickness were used. The FBG sensors were embedded in the glue layer as shown in figure 9.

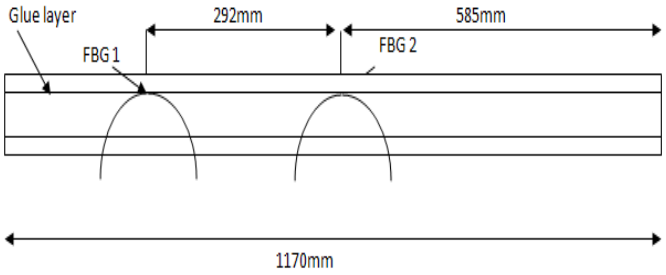

Figure 9. Placement of FBG sensors in rectanguler Beam

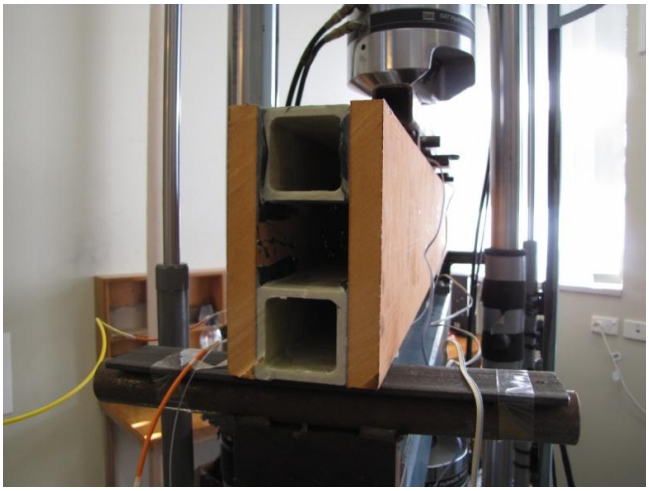

Figure 10. Prototype rectaguler beam with embedded FBG sensors

F. Experimentation

For characterization of the grating, reflected spectra were obtained using an Insensys© optical spectrum analyzer (spectral range: 1545nm -1555 nm) The FBG sensor ends were cleaved and spliced to 125µm cladding and 5µm core patch leads with E2000 connectors for connection to the spectrum analyser. Static and fatigue test were done on a MTS 100kN material testing machine under controlled environment

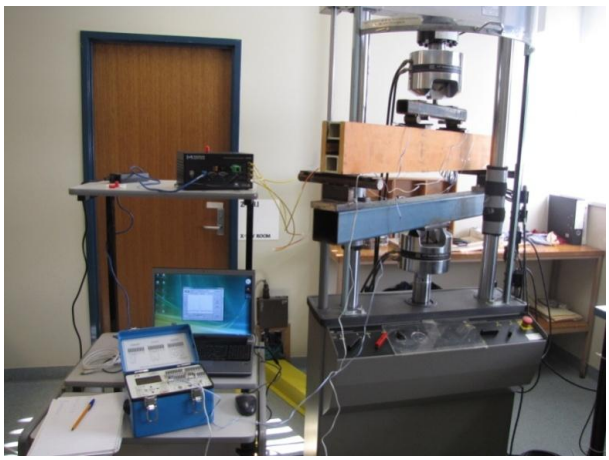

Figure 11. Beam on MTS for 4 point flexurel testing

Four point flexure tests were done according to the test setup shown in Figure 11. FBG and strain gauge responses were recorded when those were under tension and compression loads, before fatigue loading. Test sample was cycled at 20kN and stress ratio R=0.1 for 100,000 cycles while FBG's and strain gauges in tension and 50,000 cycles in compression. After each loading the sample was statically loaded and responses were recorded.

IV. Results and Discussion

A. Analytical Results

For comparison a detailed finite element model of the torsional sample was created on STRAND 7 FEA software as shown in figure 12. The model comprised with 6480 elements. The FE mesh was solved and the results were compared with the experimental results.

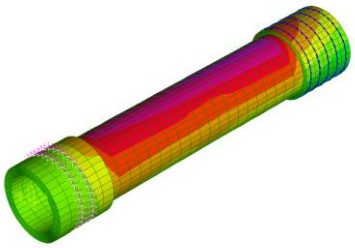

Figure 12. FEA model of the cylindrical specimen

Figure 13 shows the Principal strain, shear strain, FBG and FEA results for cylindrical specimen. Finite element results show a good agreement with the experimental results. The FBG sensor reading and FEA results of layer 5 indicated an excellent agreement. It should be noted that the FEA results are corresponding to layer 5, where the FBG sensors are embedded.

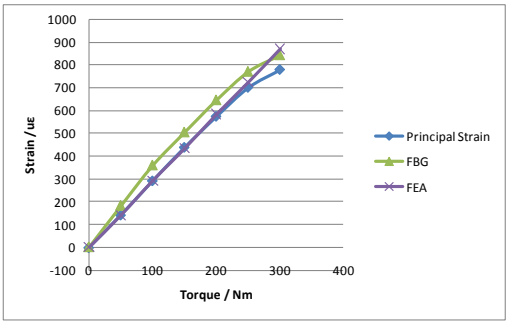

Figure 13. f FBG readings and strain gauge readings and FEA analysis results for the cylindrical specimen

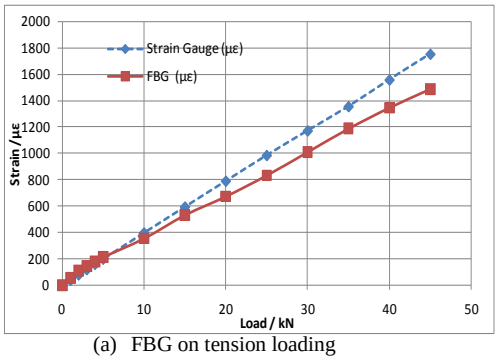

(a) FBG on tension loading

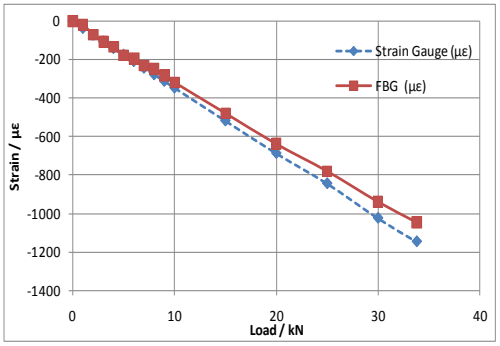

(b)FBG on compression loading

Figure 14. FBG readings with Strain gauge readings for I Beam

Figure 14 shows the comparison of FBG readings with the strain gauge reading under tension loading and compression loading for the I beam. The deviation of the readings is due to the distance between the sensors. Since the FBG sensor is placed in the glue layer, it is 6mm below the surface of the strain gauge. Interpolated strain gauge readings closely match with the FBG readings.

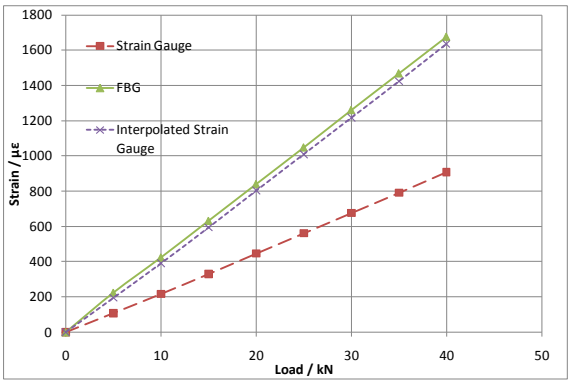

(a) FBG on tension loading

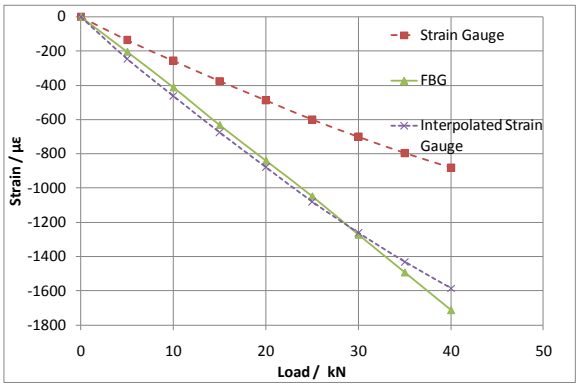

(b)FBG on compression loading

Figure 15. Comparison of FBG readings with Strain gauge readings for rectanguler Beam

The comparison of the FBG readings with the strain gauge readings for rectangular beam under tension and compression loading is given in the Figure 15. The FBG is placed directly below the strain gauge. Since the thickness of the panel is 20mm, interpolated readings were used for the comparison.

B. Comparison of FBG Readings with Strain Gauge readings after Fatigue Loading

Figure 16 shows the comparison of FBG readings with strain gauge readings after subject to 100,000 cycling load (20kN: 2kN) on tension and 50,000 cycling load (20kN: 2kN) loading on compression.

The results obtained have indicated the reliability of the FBG sensors after the fatigue cycling. There were no changes of flexural properties after 150,000 cycles of fatigue loading.

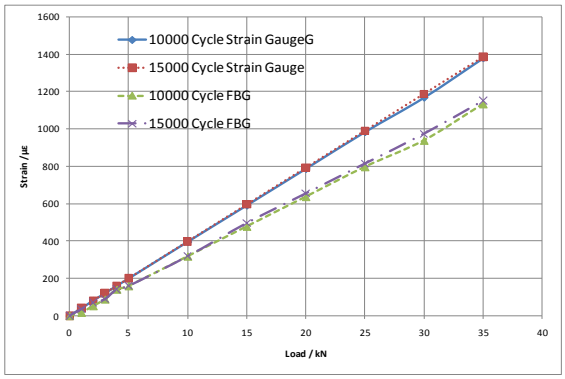

(a) FBG on tension loading

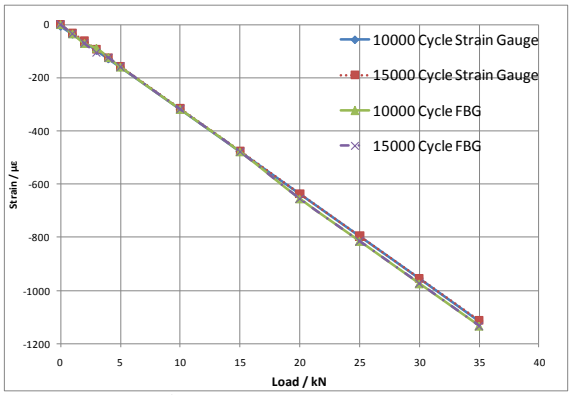

(b)FBG on compression loading

Figure 16. Comparison of FBG readings with Strain gauge readings for I Beam after fatigue.

V. Concluding Remarks

FBG sensors were successfully embedded in advanced composite structural components during the construction for the purpose of structural integrity monitoring. The performances of FBG sensors were excellent in strain measurements. Also it was found that FBG sensors which were embedded in the glue layers of composite bridge girder structure, has not shown any effect due to 150,000 fatigue cycle loading. In general, the strain measurements obtained under uniaxial, flexural, torsional and combined loading have shown an excellent agreement with the calculated values. Further investigation will be undertaken to develop FBG sensor spectral responses for development of reliable SHM system for advanced composite structures.

References

[1] A.D. Kersey, M.A. Davis, T.A. Berkoff, D.G. Bellemore, K.P. Koo, and R.T. Jones, "Progress towards the development of practical fibre Bragg grating instrumentation systems," Proceedings of SPIE 2839, SPIE, Denver, pp. 40–63, 1996.

[2] C.I. Merzbacher, A.D. Kersey and E.J. Friebele, "Fiber optic sensors in concrete structures: A review," Smart Materials and Structures, vol.5, no.2, pp. 196–208, 1996.

[3] J.A. Guemes and J.M. Menéndez, "Response of Bragg grating fibre-optic sensors when embedded in composite laminates," Composite Science and Technology, vol.62, pp. 959-966, 2002.

[4] E.N. Barton, S.L. Ogin, A.M. Thorne, G.T. Reed and B.H. Page, "Interaction between optical fibre sensors and matrix cracks in cross-ply GRP laminates- Part 1: passive optical fibres," Composite Science and Technology, vol.61, pp 1863-1869, 2001.

[5] Y. Okabe, T. Mizutani, S. Yashiro and N. Takeda, "Detection of microscopic damages in composite laminates with embedded small-diameter fibre Bragg grating sensors," Composite Science and Technology, vol.62, pp. 951-958, 2002.

[6] Y. Okabe, R. Tsuji and N. Takeda, "Application of chirped fibre Bragg grating sensor for identification of crack location in composites," Composites PartA: applied science and manufacturing, vol.35, pp. 59-65, 2004.

[7] S. Yashiro, N. Takeda, T. Okabe and H. Sekine, "A new approach to predicting multiple damage states in composite laminates with embedded FBG sensors," Composite Science and Technology, vol.65, pp 659-667, 2005.

[8] H. Ling, K. Lau, L. Cheng and W. Jin, "Viability of using an embedded FBG sensor in a composite structure for dynamic strain measurement, " Measurement, vol. 39, pp 328-334, 2006.

[9] J.A. Epaarachchi, R.C. Clegg, and J. Canning, "Investigation of the use of Near Infrared FBG (830nm) sensors for Monitoring the Structural Response of 0/90 Woven cloth/CSM Glass Fibre/Vynylester Composite under Static and Fatigue Loading," Proceedings of Health and Usage Monitoring Systems Conference, DSTO, Melbourne. 2007.

[10] J.A. Eparrachchi, J. Canning and M. Stevenson, "The response of embedded NIR (830nm) Fibre Bragg Grating (FBG) sensors in Glass Fibre Composites under Fatigue Loading," Journal of Composite Structures, 2009.

[11] P.C. Hill and B.J. Eggleton, "Strain gradient chirp of fiber Bragg gratings," Electronics Letters, vol.30, no.14, pp. 1172–1174, 1994.

[12] K. Peters, M. Studer, J. Botsis, A. Iocco, H. Limberger and R. Salathé, "Embedded optical fiber Bragg grating sensor in a nonuniform strain field: measurements and simulations," Experimental Mechanics, vol.41, no.1, pp. 19–28, 2001.

[13] S. Takeda, Y. Okabe and N. Takeda, "Delamination detection in CFRP laminates with embedded small-diameter fiber Bragg grating sensors," Composites Part A, vol.33, no.7, pp. 971–980, 2002.

[14] K. O. Hill, Y. Fujii, D. C. Johnson, and B. S. Kawasaki, "Photosensitivity in optical fiber waveguides: application to reflection fiber fabrication," Appl. Phys. Lett.vol. 32, pp.647-649, 1978.

[15] G. Meltz, W. W. Morey, and W. H. Glenn, "Formation of Bragg gratings in optical fibers by transverse holographic method," Opt. Lett., vol.14, pp. 823 -825, 1989.

D.P. Hand and E. J. Russell, "Photoinduced refractive-index changes in germanosilicate: fibres," Opt. Lett., vol.15, (2), pp.102-104, 1990.

[16] K.Raman, "Fibre Bregg gratings", Academic Press Publications, 1999.

[17] J.M. Hodgkinson, "Mechanical Testing of Advanced Fibre Composites", Woodhead Publications, 2000.